

THE ROLE OF Sr ON MICROSTRUCTURE FORMATION AND MECHANICAL PROPERTIES OF Al-Si-Cu-Mg CAST ALLOY

Mohammadreza Zamani, Salem Seifeddine, Mona Aziziderouei

Jönköping University, School of Engineering, Dept. Mechanical Engineering, Materials and Manufacturing – Casting
P.O. Box 1026, Se-551 11 Jönköping, Sweden

Keywords: Sr modification, Al-Si-Cu-Mg cast alloy, Mechanical properties, Fe-rich intermetallics, Porosity

Abstract

The aim of this paper is to assess the role of Sr modification on eutectic Si, Fe-rich intermetallic phases and porosity and their responses to the mechanical properties of a commercial high pressure die cast alloy Al-Si-Cu-Mg with Fe level up to 1%. Tensile test samples with a variety of coarsenesses, containing different Sr levels were cast using the gradient solidification technique, that enables a study of the solely influence of Sr on microstructure and tensile properties. The modification altered the morphology and size of eutectic silicon, while did not make a significant change on morphology of Fe-rich intermetallic and volume fraction distribution of porosity. The tensile test results indicate that eutectic Si modification is not a guarantee for improved mechanical properties due to the presence of a variety of intermetallics that tend to have a larger role on initiating and propagating cracks leading to premature failures in these commercial alloys.

Introduction

The automotive industry is one of the frequent users of Al-Si based foundry alloys thanks to their excellent cast-ability, high strength to weight ratio and low-cost manufacturing method [1]. Among those alloys, Al-Si-Cu-Mg cast alloys become increasingly popular due to presence of Cu and Mg in the alloys which offers distinctive advantages such as increased strength at both ambient and elevated temperature, and also responsive to heat treatment in order to achieve full potential of strength in the alloy [2, 3]. One way to improve mechanical properties of Al-Si based foundry alloys is through modification. The Al-Si eutectic consists of a hard, brittle silicon phase in a softer aluminum matrix which is the reason why most of the mechanical properties of castings, especially the elongation to fracture, are determined by the eutectic microstructure. Modification of the Al-Si eutectic from a flake-like to a fine fibrous silicon structure can be achieved in two different ways; by addition of certain elements (chemical-modification) or with a rapid cooling rate (quench-modification) [4]. One of the reputable elements that has been employed in recent years as a chemical modifier is Strontium owing to the following reasons: (a) it is easy to handle, (b) it has good modification rate, (c) it has long incubation period and (d) its fading effect is low. It was conceived addition of a few hundred parts per million Sr modifies the eutectic Si morphology from coarse plate-like into fine fibrous and have a beneficial effect on both strength and ductility. Unfortunately, modification has also been associated with negative side effects such as porosity and hot tearing and is not always a recommended procedure. The increased porosity often causes a reduction in mechanical properties compared with the unmodified alloy, even though the silicon has become modified. Although many theories have been proposed to account for these effects, most can be considered

inadequate because of their failure to resolve contradictions and discrepancies in literatures. On top of that, amount and characteristics of porosity are decisive factors playing role in mechanical properties of cast component [5-8]. The present study aims to investigate the solely effect of Sr modification on the microstructural formations including porosity and resulting mechanical properties of Al-Si-Cu-Mg cast alloys, and also to recommend a proper Sr level for optimum modification based on the coarseness of microstructure of alloys.

Experimental Methods

Ten kilograms of EN AC 46000 commercial Al-alloy ingots were melted in a resistance furnace with a silicon carbide crucible at 750°C. Then melts were modified with Sr using Al-10%Sr master alloy. The addition was carried out by placing Al-10%Sr master alloy particle on the melt surface and twenty minutes was considered for dissolution of strontium. Chemical composition of each samples was obtained by optical emission spectroscopy, and the data is summarized in Table 1.

Table 1. Chemical compositions of the alloys
(wt.% except for Sr ppm)

	Si	Cu	Fe	Mg	Zn	Mn	Sr	Al
Alloy 1	8.02	2.11	0.78	0.26	0.99	0.17	0	Bal.
Alloy 2	8.02	1.89	0.92	0.26	1.03	0.21	37	Bal.
Alloy 3	8.05	1.90	0.91	0.26	1.05	0.21	68	Bal.
Alloy 4	8.10	2.02	0.90	0.25	0.96	0.24	150	Bal.
Alloy 5	8.30	1.99	0.98	0.27	1.06	0.21	276	Bal.
Alloy 6	8.21	1.95	0.98	0.27	1.07	0.21	486	Bal.

Cylindrical rods (length 18 cm, diameter 1 cm) were cast in a 200°C preheated permanent mold and subsequently were remelted with the gradient solidification technique. The rods were inserted into the furnace at 710°C where they were remelted for 20 min. The furnace was then raised with a prescribed speed and the samples were draw from the furnace. The speed of the furnace determines the solidification rate of the samples; different microstructures can thereby be produced by changing the speed. Three different coarsenesses of the microstructure having SDAS of approximately 10, 25 and 50 μm , were produced for the present investigation. Water cooling beneath the furnace was used for high furnace speeds, 3 mm/s and 0.3mm/s corresponding to SDAS of 10 and 25 μm respectively, to cool the samples whereas no water cooling was used for the 0.03 mm/s velocity that corresponds to SDAS of 50 μm . Since the solidification is directional, the samples produced possess low degree of defects and impurities. Tensile test bars were prepared out of the rods and then tensile test was performed in room temperature at a constant strain rate of 0.5 mm/min [9]. The tensile fracture characteristics

were examined using optical microscopy. The optical microscope was used to probe the longitudinal sections as well as cross-sectional ones near the fractured surfaces in order to investigate tensile fracture characteristics. In order to determine the volume fraction of porosity, mass density of each sample for different conditions were measured via buoyancy method by means Mettler Toledo machine. Quantity of porosity (ϕ) was obtained from equation 1,

$$\phi = (\rho_0 - \rho_C) / \rho_0 \quad (1)$$

where ρ_0 is the mean density value of samples having 10 μm SDAS since they obtained highest density value among others, and ρ_C is density value of each sample. An image analysis system (IAS) via qualitative technique was utilized to study modification level of samples based Djurdjevic's methods [8].

Results and Discussion

1 - Influence of Sr modification on microstructure and porosity

There are many theories trying to explain the role of Sr on the modification of eutectic silicon in Al-Si alloys [4, 10, 11]. Among the widely accepted theories, the theory of Lu and Hellawell, is based upon impurity-induced twinning mechanisms. The theory claims that Sr could act as a poison to already growing atomic layers. Sr is assumed to adsorb to the step or kink sites, thus preventing attachment of atoms or molecules to the crystal. Further this corrupting atoms could induce twinning by altering the stacking sequence of atomic layer in order to grow around the impurity [4].

The microstructure variations of the samples obtained under different cooling rates, 10, 25 and 50 μm in SDAS, are presented as a function of the Sr level in Figure 3. In a general view, the microstructure is a mixture of aluminum dendrites surrounded by the Al-Si eutectic aggregate and some intermetallic phases. As depicted in Figure 3 a, b and c, the microstructure in the unmodified samples contains coarse plate-like silicon that often radiates from polyhedral silicon particles. Although an increased cooling rate refined the microstructural constituents and degraded eutectic silicon in size, it was unable to change plate-like shape of eutectic silicon, see the microstructure in Figure 3. Only by adding 35 ppm Sr, the silicon shape in samples with SDAS up to 25 μm experienced a major change. In order to obtain similar structural heterogeneity, samples with SDAS 50 μm require at least 150 ppm Sr, as revealed in Figure 3 l. Only above these levels, 35 ppm for finer and 150 ppm for coarser structures, eutectic silicon is dramatically reduced and the morphology is coral like proving that Sr can refine the eutectic silicon from acicular to fibrous even if the eutectic phase is encompassed with bunch of intermetallic compounds. Different Sr levels lead to different extent of morphology change, depending on the coarseness of microstructure, see Figure 3 d-r; nevertheless, a clear progressive trend of silicon modification level can be observed in samples having 50 μm SDAS. At levels of 150 ppm and structures of 50 μm in SDAS, there still exist regions containing a bimodal distribution of silicon, in which typically fine fibrous silicon are accompanied by coarse or even plate-like. In order to achieve a complete modification of Si for these coarsest microstructures, an addition of at least 280 ppm is required. However, when Sr addition is increased to 500 ppm, the result is almost the same as that of 280 ppm, but excess Sr might generate $\text{Al}_2\text{Si}_2\text{Sr}$ compounds in the microstructure and

consequently degrades the alloy performance, as stated in literature [12]. Modification levels of eutectic silicon for each sample were calculated according to Djurdjevic's method [8] and the results were depicted in Figure 1.

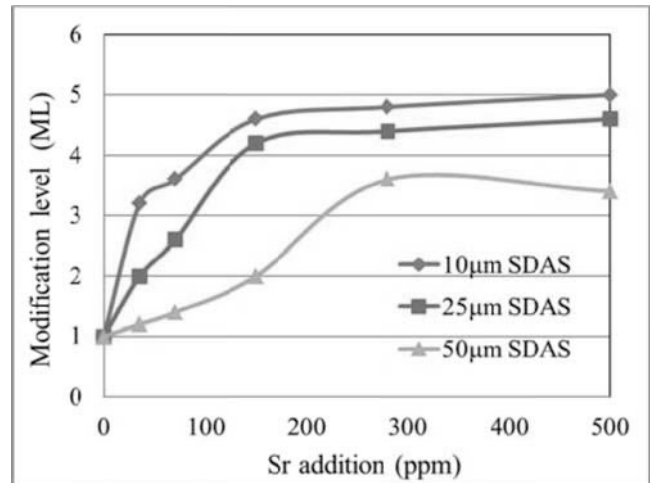


Figure 1. Effect of Sr content on Modification level of the alloy having different SDAS

Unlike the eutectic silicon, Sr did not make any significant change on morphology of various intermetallic phases present in the alloy such as $\beta\text{-AlFe}_5\text{Si}$, $\alpha\text{-Al}_5(\text{Fe}, \text{Mn})_3\text{Si}_2$, $\theta\text{-Al}_2\text{Cu}$, $\pi\text{-Al}_8\text{FeMg}_3\text{Si}_6$ and etc, Figure 2, the phases were recognized through comparing with similar study of [13]. Size and spatial distribution of the intermetallic compounds were mainly dependent on cooling rate and consequently SDAS, as it is clear in Figure 3 a, b and c. In fact, increased cooling rate will lead to achieve reduced size of the compounds, since the time available for growth is decreased [14].

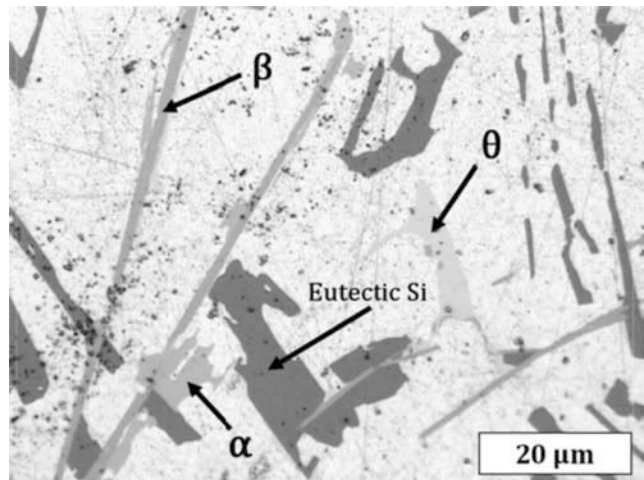


Figure 2. Intermetallic phases found in unmodified alloy having 50 μm SDAS

Modification as well as solidification rate play an important role in volume fraction and characteristic of defects such as gas porosity and shrinkage cavity [7, 15]. As it was indicated, volume fraction of porosity was measured for unmodified and modified samples having different SDAS via buoyancy method. It is worth to bear in mind is that the melt hydrogen content has not been

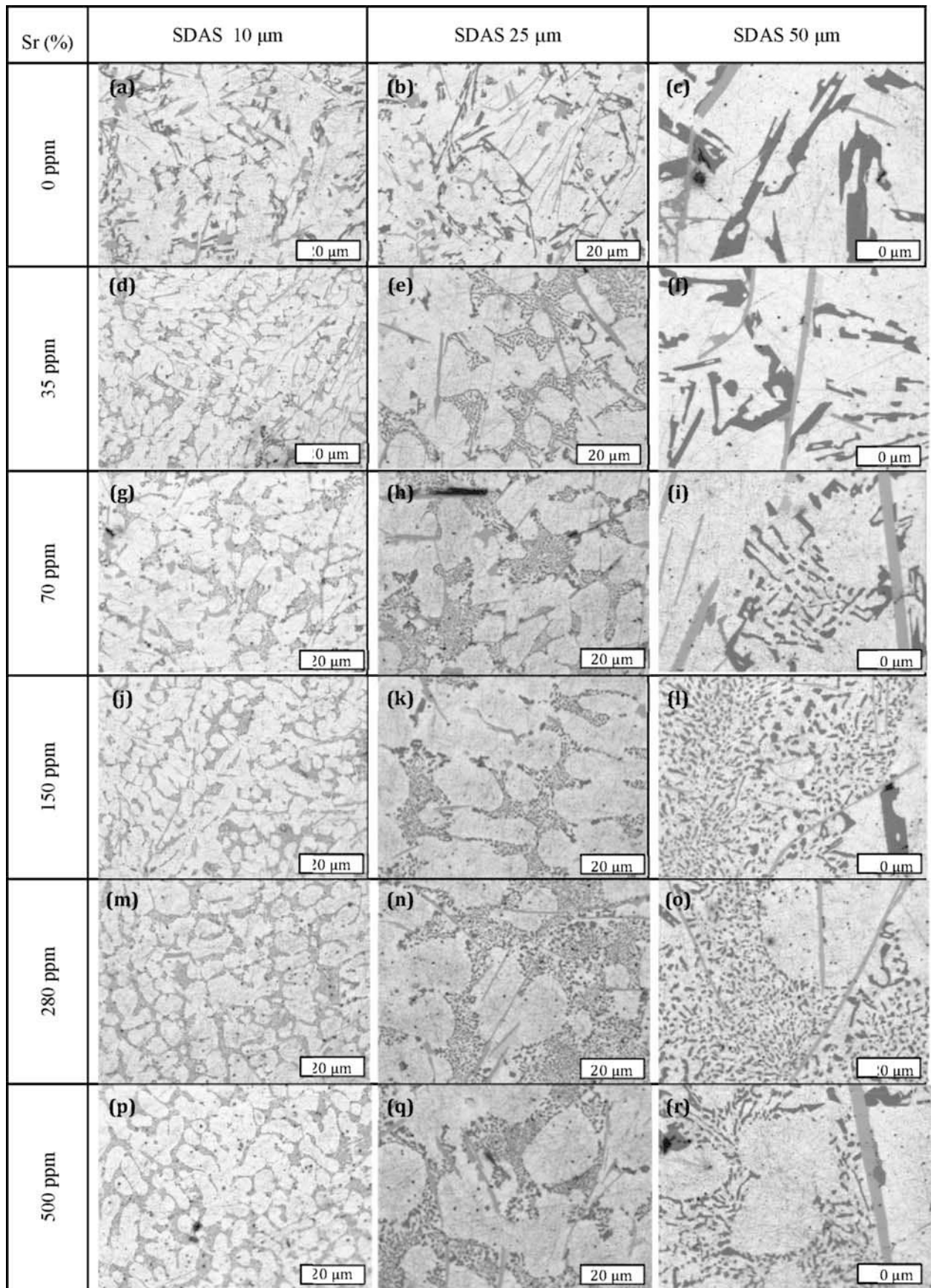


Figure 3. Microstructural evolution of unmodified and modified alloy solidified within different cooling rates; from left to right SDAS is increasing, from top to bottom Sr content is increasing

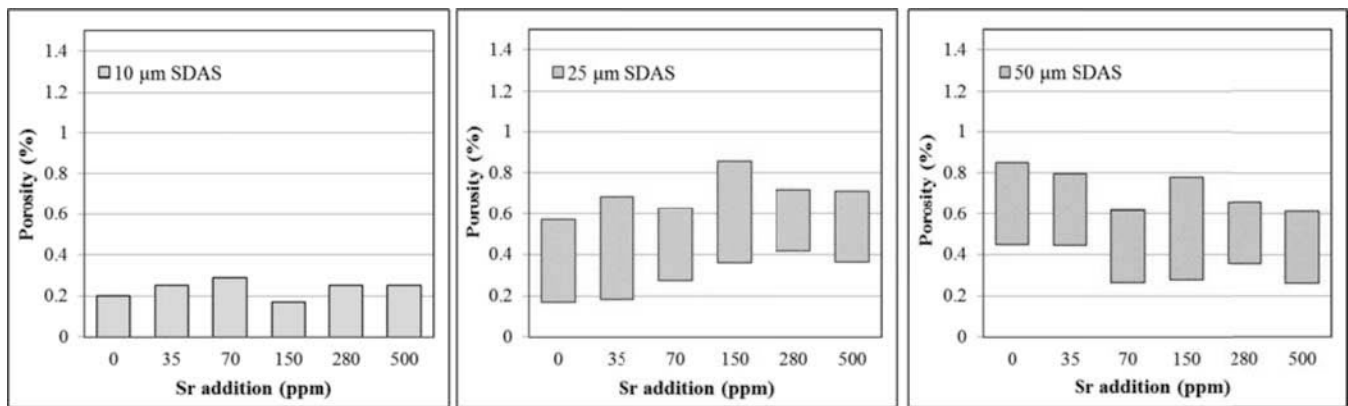
measured and assumed in this case to be constant for all the alloys since they have been produced under similar conditions. A general observation indicates, see Figure 4, that porosity values for all conditions are relatively low, less than 1%, which is due to the mode of solidification as a result of using gradient solidification technique. Samples are solidified in directional manner and a major part of the impurities are pushed ahead the advancing solidification front which are lately cut and not being a part of the evaluated samples. In addition, the current study cannot reveal any trend in porosity level as a function of Sr, no matter the size of SDAS, which is in agreement with the a study by Dinnis et al [15].

As depicted from , as the solidification time is short, small SDAS, less time will be available for the diffusion of the hydrogen into the interdendritic regions which results in lower pore volume fraction. Theories of oxide films suggest that when an oxide film is approached by the solidification front, the particle experiences the hydrogen-rich environment produced by the rejection of gas from the advancing solid. Furthermore, the access of gas by diffusion into the air pocket in the gap of the oxide particles, the pore will starts to form and grow. As the freezing rate becomes slower, higher SDAS, and the particle is poorly wetted by the melt, time will therefore be available for more hydrogen to diffuse resulting in pore expansion and growth resulting as well in larger pore volume fractions as indicated from the measurements in the current study [16, 17]. Comparing the pore volume fractions, the samples with SDAS 25 and 50 μm are associated with largest fraction of porosity which might be due to the arrestment of premature pores as they become entrapped by the advancing solidification front, irrespective to the Sr content.

2- Effect of Modification on Mechanical properties and fracture Analysis of The Alloy

A silicon is refined by the additions of Sr there exist no evidence that the iron-rich intermetallics have been influenced by the modification treatment. These observations are confirmed by qualitatively studying the microstructures in Figure 3. As clearly demonstrated, the smaller the SDAS the finer and more homogenous is the microstructure and vice versa. The fracture profile of smallest SDAS is of more transgranular character, while for higher SDAS > 50 μm the fracture profile seems to be more intergranular; as depicted from figure Figure 3 c, f, i, l, o and r, the iron-rich compounds are formed as coarse and large platelets with a random orientation.

In most of all ductile materials that are subjected to monotonic loading, the progression of damage is devoted to the nucleation and growth of cracks. The release of stresses that is carried by the second phase particles such as Si and intermetallic compounds, at a macroscopic level when cracking occurs, affects the overall load bearing capacity of the material. When the cooling rate is high, the silicon is modified partially due to cooling conditions itself, but also due to the Sr additions. The overall microstructure is also refined as a result of fast cooling. As the size of intermetallics is kept fine and constant, the influence of Sr is evident on the Si refinement which directly impact on the elongation to fracture where the fracture seems to be transgranular. The reduction in elongation to fracture for the material with larger SDAS might be devoted to the larger Si particles with flake like morphology and to the large iron-rich needles or platelets. Since Sr modification did not impact on the size and morphology of the iron-rich intermetallics, it seems that these phases are controlling to a major extent the fracture behaviour. The fracture profile indicates that the fractures in samples with SDAS 20 seem to follow the particle orientations and exhibiting a mixed mode failure. In most cases, the fracture is dominated by the iron-rich intermetallics, Figure 5 b, e, h, k, n and q, and silicon particles, and for the coarser microstructure, SDAS 50, the fracture seems solely of a intergranular failure mode where the iron rich phase play a dominant role. Being hard and brittle, these needles tend to have relatively low bond strength to the matrix and as noticed from the fracture profiles in fig x, there are no doubts that the iron-rich intermetallics together with the silicon particles have been participating in the damage events. Both seem to play a critical role in the crack initiation and propagating processes, acting as easy crack paths, linking the particle fractures together and leading to an uncontrolled fracture of the material. In these cases, the role of Sr on elongation to failure is absent, instead iron-rich particles has to be neutralized by a proper corrector, normally Mn [18]. The tensile strength depends also on the overall fineness of the microstructure. A non-modified structure with SDAS 10 possesses finer and rounder silicon than non-modified structure where SDAS is 50. The overall structure differences are directly impacting on the tensile strength as depicted in Figure 7 . As silicon is modified, the tensile strength is slightly improved but not to the same extent as the elongation to fracture, see diagrams in Figure 6 and 7.



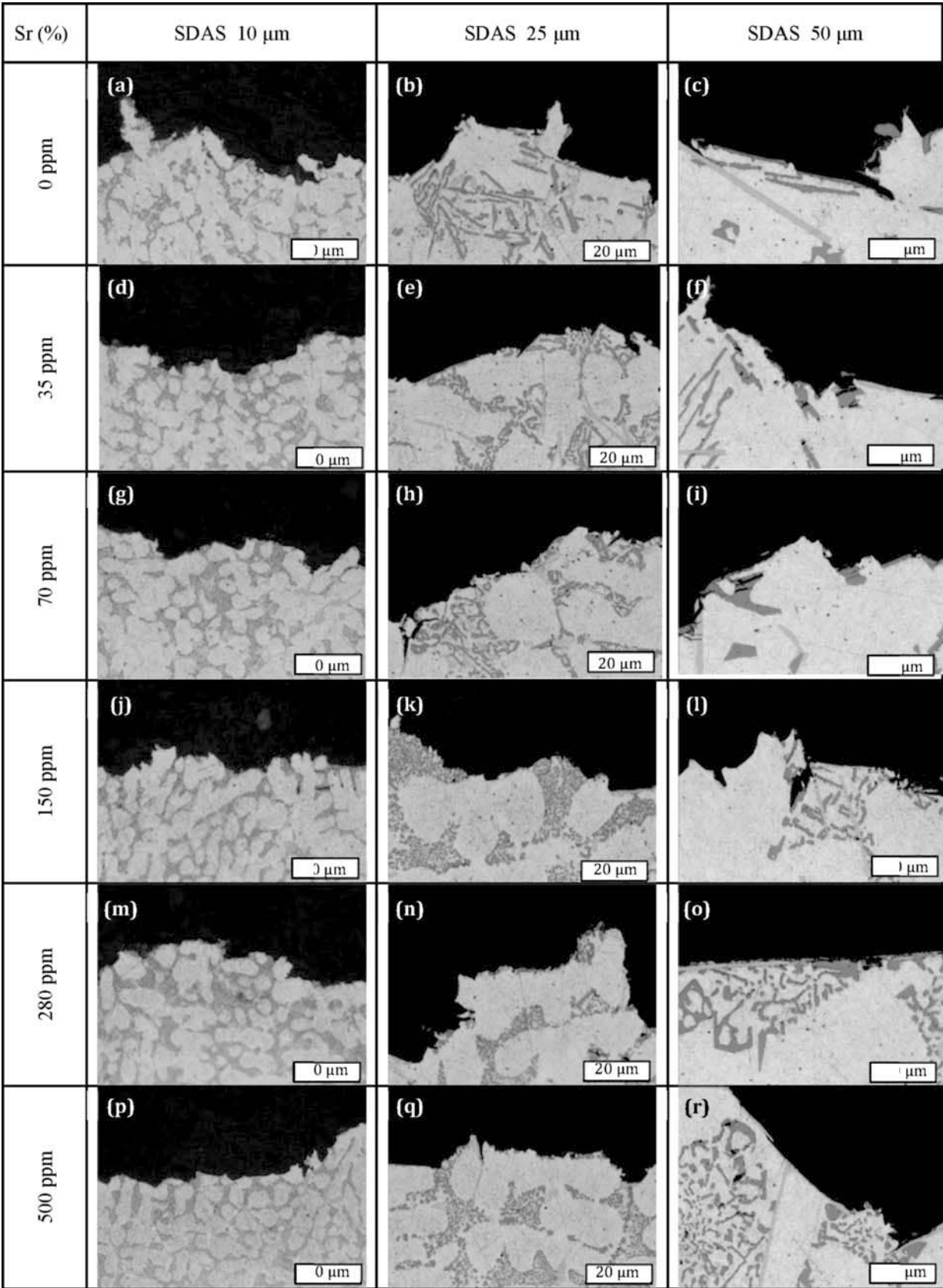


Figure 5. Fracture profile of unmodified and modified alloy solidified within different cooling rates; from left to right SDAS is increasing, from top to bottom Sr content is increasing

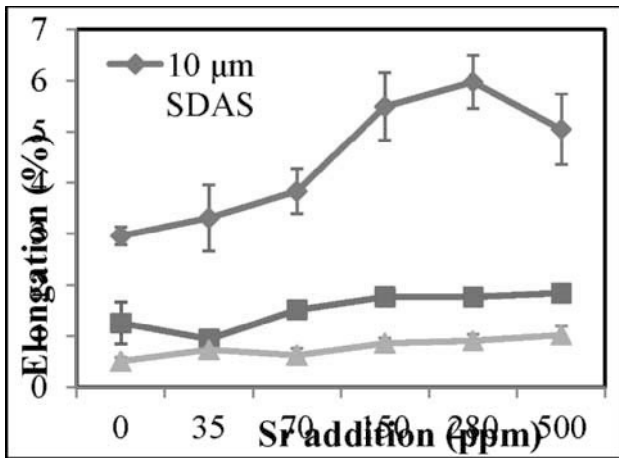


Figure 6. Effect of Sr content and cooling rate on elongation

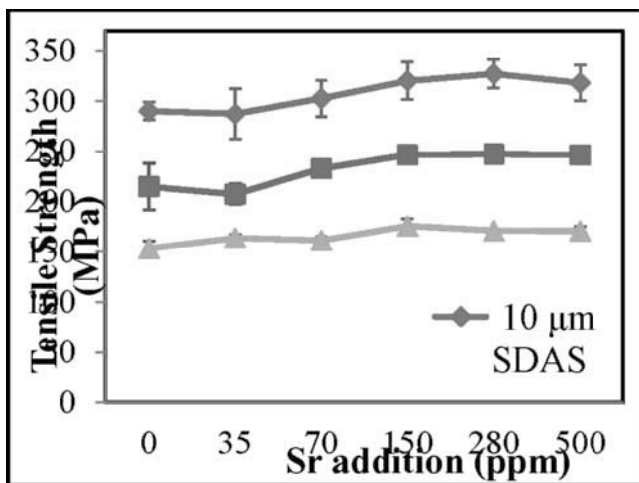


Figure 7. Effect of Sr content and cooling rate on UTS

Conclusion

The following conclusions can be made:

- Microstructures with SDAS < 10 μm is fully modified with only 35 ppm Sr while higher level of Sr are required for coarser microstructure. For microstructures with SDAS > 50 μm, 150 ppm is a minimum value to achieve a reasonable modification
- There are no indications that the Fe-rich intermetallics are affected by Sr additions.
- Porosity volume fractions are mostly cooling rate dependent rather than modification level related.
- Highly modified samples with SDAS 10 μm offered the highest elongation to fracture values.
- The strength of the modified alloys is a function of the overall coarseness of the microstructure.
- Al-Si modification is not a guarantee for realizing higher ductility in EN AC 46000 alloys; although samples with SDAS of 25-50 μm were highly modified, the Fe-rich intermetallics govern the elongation to fracture.

References

1. Kaufman, J.G., *Introduction to aluminum alloys and tempers* 2000: Asm Intl.

2. Caceres, C. and J. Taylor, *Enhanced ductility in Al-Si-Cu-Mg foundry alloys with high Si content*. Metallurgical and Materials Transactions B, 2006. **37**(6): p. 897-903.
3. Gowri, S. and F. Samuel, *Effect of alloying elements on the solidification characteristics and microstructure of Al-Si-Cu-Mg-Fe 380 alloy*. Metallurgical and Materials Transactions A, 1994. **25**(2): p. 437-448.
4. Lu, S.Z. and A. Hellawell, *The mechanism of silicon modification in aluminum-silicon alloys: impurity induced twinning*. Metallurgical and Materials Transactions A, 1987. **18**(10): p. 1721-1733.
5. Ceschini, L., et al., *Effect of Fe content and microstructural features on the tensile and fatigue properties of the AlSi10Cu2 alloy*. Materials & Design, 2011.
6. Dinnis, C., et al., *The influence of strontium on porosity formation in Al-Si alloys*. Metallurgical and Materials Transactions A, 2004. **35**(11): p. 3531-3541.
7. Lu, L., et al., *Eutectic solidification and its role in casting porosity formation*. JOM Journal of the Minerals, Metals and Materials Society, 2004. **56**(11): p. 52-58.
8. Djurdjevic, M., H. Jiang, and J. Sokolowski, *On-line prediction of aluminum-silicon eutectic modification level using thermal analysis*. Materials characterization, 2001. **46**(1): p. 31-38.
9. Handbook, A.S.M.M., *Metals Park*. Ohio: American Society for Metals, 1972.
10. Thall, B.M. and B. Chalmers, *Modification in Aluminium Silicon Alloys*. Journal of the Institute of Metals, 1950. **77**(1): p. 79-&.
11. Davies, V.D.L., *Direct Microscopic Observation of Solidification of Metals*. Journal of the Institute of Metals, 1963. **92**(4): p. 127-&.
12. Zarif, M., B. McKay, and P. Schumacher, *Study of heterogeneous nucleation of eutectic Si in high-purity Al-Si alloys with Sr addition*. Metallurgical and Materials Transactions A, 2011. **42**(6): p. 1684-1691.
13. Ceschini, L., et al., *Microstructure, tensile and fatigue properties of the Al-10% Si-2% Cu alloy with different Fe and Mn content cast under controlled conditions*. Journal of Materials Processing Technology, 2009. **209**(15): p. 5669-5679.
14. Seifeddine, S., S. Johansson, and I.L. Svensson, *The influence of cooling rate and manganese content on the β-Al₅FeSi phase formation and mechanical properties of Al-Si-based alloys*. Materials Science and Engineering: A, 2008. **490**(1): p. 385-390.
15. Dinnis, C.M., et al., *The influence of strontium on porosity formation in Al-Si alloys*. Metallurgical and Materials Transactions a-Physical Metallurgy and Materials Science, 2004. **35A**(11): p. 3531-3541.
16. Campbell, J., *Castings* 2003: Butterworth-Heinemann.
17. Shih, T.S., L.W. Huang, and Y.J. Chen, *Relative porosity in aluminium and in aluminium alloys*. International Journal of Cast Metals Research, 2005. **18**(5): p. 301-308.
18. Shabestari, S.G., et al., *Effect of Mn and Sr on intermetallics in Fe-rich eutectic Al-Si alloy*. International Journal of Cast Metals Research, 2002. **15**(1): p. 17-24.